Measurement: Energy 3 (2024) 100017

Contents lists available at ScienceDirect

Measurement: Energy

journal homepage: www.sciencedirect.com/journal/measurement-energy

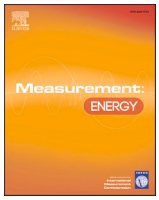

Regular Paper

# A quantitative comparison of economic viability, volatile organic compounds, and particle-bound carbon emissions from a diesel engine fueled with biodiesel blends

Abdulfatah Abdu Yusuf [a,*], Ibham Veza [b], Zubeda Ukundimana [c], Adolphus Nippae [a], Charles Asumana [d], Eric Kay Jebboe Jr. [a], M.A. Mujtaba [e], Islam Md Rizwanul Fattah [f], Manzoore Elahi M. Soudagar [g]

[a] College of Engineering, University of Liberia, P. O. Box 10-9020, 1000, Monrovia, Liberia
[b] Department of Mechanical Engineering, Universiti Teknologi Petronas, Seri Iskandar, 32610, Malaysia
[c] Department of Mechanical Engineering, University of Rwanda, P.O. Box 3900, Kigali, Rwanda
[d] Thomas J.R. Faulkner College of Science, Technology, Environment and Climate Change (CoSTECC), University of Liberia, P. O. Box 10-9020, 1000, Monrovia, Liberia
[e] Department of Mechanical, Mechatronics and Manufacturing Engineering (New Campus), University of Engineering and Technology Lahore, 54000, Pakistan
[f] Centre for Technology in Water and Wastewater, School of Civil and Environmental Engineering, Faculty of Engineering and IT, University of Technology Sydney, Ultimo, NSW, 2007, Australia
[g] Faculty of Engineering, Lishui University, 323000, Lishui, Zhejiang, China

ARTICLE INFO

*Keywords:*
Biodiesel
Environmental sustainability
Economic analysis
Emissions
Diesel engine

ABSTRACT

Despite the environmental advantages of biofuel blends, detailed studies on emissions of polycyclic aromatic hydrocarbons (PAHs), n-alkanes, and particle-bound carbon from diesel engines, particularly when fueled with biodiesel, remain limited. This study addresses these gaps by analyzing biodiesel blends from neem, linseed, and jatropha oils produced via mechanical extraction and assessing their impact on volatile organic compounds and particle-bound carbon emissions in diesel engine. Economic evaluations of production costs, engine modifications, and payback periods are also conducted. The result shows that jatropha biodiesel exhibits a calorific value of 35.7 MJ/kg, while neem biodiesel shows superior oxidative stability due to its low iodine value. Additionally, linseed biodiesel displays favorable cold flow properties due to its high density and cetane value. Compared to D100, the N10 and N30 blend notably reduced high molecular weight PAH emissions by 10.7 % and 38.4 %, respectively, with the N30 blend achieving a remarkable 76 % reduction in formaldehyde emissions. Conversely, the J10 blend increased specific PAHs, while the J30 blend reduced PAHs by 21.3 %. Both L10 and L30 blends showed reduced naphthalene emissions, with the J30 blend notably reducing elemental carbon (EC) by 31.4 %, although organic carbon (OC) slightly increased. In contrast, the N30 blend decreased both EC and OC emissions, demonstrating a dose-dependent relationship between biodiesel concentration and emissions reduction. Overall, Jatropha biodiesel blends offer the best balance of economic efficiency and emission reductions, resulting in shorter payback periods and lower carcinogenic risks. Neem and linseed blends also provide environmental benefits but with varying economic implications, highlighting the trade-offs between production costs and long-term sustainability.

## 1. Introduction

The global demand for sustainable and environmentally friendly energy sources has driven extensive research into alternative fuels. Among these, biodiesel has garnered significant attention due to its potential to reduce greenhouse gas emissions (GHGs), enhance energy security, and provide a renewable substitute for petro-diesel [1]. Biodiesel is derived from various biological feedstocks, including vegetable

* Corresponding author.
*E-mail addresses:* yusufaa@ul.edu.lr (A.A. Yusuf), ibham.veza@utp.edu.my (I. Veza), ukundimanaa@yahoo.fr (Z. Ukundimana), nippaead@ul.edu.lr (A. Nippae), asumanach@ul.edu.lr (C. Asumana), eric.jebboe@student.ul.edu.lr (E.K. Jebboe), m.mujtaba@uet.edu.pk (M.A. Mujtaba), islammdrizwanul.fattah@uts.edu.au (I.M. Rizwanul Fattah), manzoor@lsu.edu.cn (M.E.M. Soudagar).

https://doi.org/10.1016/j.meaene.2024.100017
Received 8 July 2024; Received in revised form 19 August 2024; Accepted 19 August 2024
Available online 25 August 2024

oils and animal fats, through a transesterification process that converts triglycerides into fatty acid methyl esters [2–4]. However, biodiesel's efficiency and environmental impact depend significantly on the feedstock used, necessitating a thorough investigation of different biodiesel sources.

In recent years, extensive research efforts have focused on characterizing the physicochemical properties of biodiesel derived from various feedstocks [5–7]. These properties, including density [8], viscosity [9], calorific value, flash point [10], and cetane number [11], influence biodiesel's combustion characteristics [12], engine performance, and emissions profile [13]. Among the variety of biodiesel feedstocks, neem, linseed, and jatropha oils have garnered considerable attention due to their abundance, accessibility, and favorable properties for conversion into biodiesel. Neem, linseed, and jatropha oils are promising biodiesel feedstocks due to their unique fatty acid compositions and environmental benefits. Neem oil is rich in oleic acid and is known for its favorable cetane number and viscosity, potentially leading to improved combustion characteristics [14]. Linseed oil is characterized by high levels of polyunsaturated fatty acids and offers enhanced cold flow properties, making it suitable for use in colder climates [15]. With a balanced fatty acid profile, Jatropha oil presents a compelling case for biodiesel production due to its oxidation stability and superior cold flow properties [16].

While biodiesel presents a promising alternative to petroleum-based diesel, its adoption still faces several challenges and limitations. Variability in feedstock composition, production methods, and fuel properties necessitates comprehensive analysis and optimization to ensure consistent performance and compatibility with existing engine technologies. Additionally, the literature concerning a comprehensive investigation into the emissions of polycyclic aromatic hydrocarbons (PAHs), n-alkanes, and particle-bound carbon in diesel engines, particularly when fueled with biodiesel and diesel blends, remains underexplored. A significant proportion of existing studies have predominantly centered their attention on conventional pollutants such as nitrogen oxides (NOx), hydrocarbons (HC), carbon monoxide (CO), and smoke emissions [13,17–21]. While these pollutants are undeniably critical markers of combustion efficiency and air quality, the limited attention given to PAHs, n-alkanes, and particle-bound carbon emissions leaves a considerable void in our understanding of the full environmental impact of alternative fuel utilization.

PAH emissions are known for their carcinogenic and mutagenic properties and pose a substantial environmental and health risk [22]. Similarly, n-alkanes contribute to the complex composition of exhaust emissions and merit scrutiny due to their implications for air quality [23]. Additionally, particle-bound carbon emissions are directly linked to the formation of particulate matter, a critical factor in air quality degradation and respiratory issues [24]. Neglecting these components could be a significant oversight, as they contribute to atmospheric pollution and pose potential health hazards that necessitate comprehensive investigation [12].

This study aims to fill the existing research gaps by conducting a comprehensive analysis of the fuel properties and particulate emissions of biodiesel blends made from neem, linseed, and jatropha oils. Through the use of a common rail direct injection (CRDI) diesel engine, the research investigates the effects of various biodiesel blend ratios on particulate-bound carbon, volatile organic compounds (VOCs), n-alkanes, and polycyclic aromatic hydrocarbons (PAHs). Additionally, the study evaluates the economic implications of these biodiesel blends. The results will provide valuable insights into the environmental and health impacts of non-edible oil biodiesel alternatives, offering essential data to support the advancement of cleaner, more sustainable diesel fuels.

## 2. Methodology

### 2.1. Biodiesel production and fuel properties

#### 2.1.1. Extraction of oil from neem, linseed, and jatropha

The oil extraction process can be categorized into mechanical or solvent extraction methods. In this study, the mechanical method was chosen, which is known for its traditional domestic usage and is recognized as the easiest and quickest way to obtain oil samples from various oil-bearing seeds. Before extraction, it is necessary to remove any metal pieces in the seeds to avoid damage to the screw press. Then, the seeds are transferred through the opening inside the barrel. When the screw shaft is rotated by the motor, the seeds are carried forward and compressed against the outer lining of the barrel. At the same time, the pressure increases as the cavity volume of the screw shaft decreases and the extracted oil flows out from the slots of the chamber. The extracted oil was then collected, and each of the oil was placed in two different centrifuge tubes. 5 mL of oil was added to a 15 mL centrifuge tube and centrifuged at 3500 rpm for 5 min. The purpose of performing this process is to remove any impurities and unwanted materials in the sample. After centrifugation, a better separation of the oil and the residues was obtained. This assists in determining the exact amount of the right oil representative that can be used for further tests.

#### 2.1.2. Transesterification process

In the transesterification process, neem, jatropha, and linseed oils are individually subjected to a series of steps to produce biodiesel. Initially, each oil is heated on a hot plate within a temperature range of 65–70 °C for 1 h, ensuring uniform heating through continuous stirring. This heating step reduces the viscosity of the oils, facilitating a more effective reaction with methanol.

Once heated, the oils are filtered through filter paper to remove any particulates and impurities. Each filtered oil is then mixed with hot distilled methanol at a molar ratio of 4:1 (methanol to oil) and a catalyst, typically sodium hydroxide (NaOH), in a concentration of 1 % by weight of the oil. This mixture is maintained at the reaction temperature under constant stirring for a predetermined time, typically 60 min, to ensure a complete reaction.

After the reaction period, the mixture is allowed to cool to room temperature. To neutralize any remaining acid and aid in phase separation, 0.5 % w/w of solid sodium carbonate ($Na_2CO_3$) is introduced and stirred into the mixture. Then, the mixture is allowed to settle for 1 h, resulting in the formation of two distinct layers. The upper layer is the biodiesel, while the lower layer consists of glycerin. The biodiesel and glycerin layers are separated using a separating funnel. The glycerin, being the denser phase, is removed and set aside. The biodiesel is then subjected to a washing process with water. This involves washing the biodiesel with an equal volume of distilled water multiple times until the wash water is clear, indicating the removal of residual methanol, soap, and other impurities.

Finally, the biodiesel is dried to remove any remaining water. This is achieved by heating the biodiesel to 100 °C under a vacuum or by using a drying agent. The final product is then filtered to remove any residual particles, resulting in purified biodiesel ready for use.

#### 2.1.3. Description of analytical instruments and measurement techniques

Table 1 provides a comprehensive overview of the instruments used for measuring various properties of biodiesel fuels, detailing the specifications and measurement conditions. The density of the fuels is measured using a digital density meter with high precision, boasting an accuracy of ±0.0001 g/cm$^3$ within a range of 0–3 g/cm$^3$ and an uncertainty of ±0.05 %. A small sample amount of 2 mL is required for this measurement. The calorific value, which indicates the energy content of the fuel, is determined using an automatic bomb calorimeter with a fast response time of under 4 s and high linearity of less than 0.08 % per 5 °C, providing a resolution of 0.0001 °C. The ignition time for this

**Table 1**
Specifications and instrumentation for fuel property measurements.

| Property | Instrument | Details |
|---|---|---|
| Density, g/cm$^3$ | Digital density meter | Accuracy: ±0.0001 g/cm$^3$; Range: 0 g/cm$^3$ to 3 g/cm$^3$; Uncertainty: ±0.05 %; Sample amount: 2 mL. |
| Calorific value, J/g | Automatic bomb calorimeter | Response time: <4 s; Linearity: <0.08 % per 5 °C; Resolution: 0.0001 °C; Ignition time: 5 s. |
| Kinematic viscosity, (cSt) | Automatic kinematic viscometer | Range: 0.5 cSt to 25000 cSt; Flow time: 0.001 s; sample amount: 10 mL–15 mL; Temp sensitivity: 0.001 °C. |
| Flash point, °C | Pensky-Martens apparatus | Range: 40 °C to 360 °C; Accuracy: ±0.1 °C. |

measurement is 5 s. Kinematic viscosity, an important parameter for assessing the fluidity of the fuel, is measured using an automatic kinematic viscometer. This instrument covers a wide range of viscosities from 0.5 cSt to 25000 cSt and requires a sample volume of 10–15 mL. It has a flow time resolution of 0.001 s and is sensitive to temperature changes as small as 0.001 °C. Finally, the flash point, which indicates the temperature at which the fuel can vaporize to form an ignitable mixture, is measured using Pensky-Marten's apparatus. This device accurately measures flash points within a range of 40 °C–360 °C with a precision of ±0.1 °C.

#### 2.1.4. Gas chromatography-mass Spectrometry (GC-MS) analyses

In the GC-MS analyses of oil sample properties, the experiment commenced by weighing 5 mg of the oil sample and dissolving it in 1 mL of hexane. An extraction step was omitted due to the relatively clean nature of the sample. Subsequently, the sample underwent derivatization by adding 100 μL of N, O-Bis(trimethylsilyl)trifluoroacetamide (BSTFA) to enhance the separation of polar compounds. The GC-MS instrument was equipped with a 30 m × 0.32 mm x 0.25 μm DB-5 film column, set to an initial temperature of 50 °C, held for 2 min, then ramped at 5 °C/min to 250 °C, and held for 5 min. The injection was performed in splitless mode with a 1 μL sample volume. Mass spectra were collected in the range of 50–500 *m/z*. Data analysis was conducted using the instrument's software, and compounds were identified based on mass spectra and retention times. Quantification was achieved using calibration standards.

### 2.2. Engine setup and procedure

#### 2.2.1. Test setup

The experimental setup utilized an in-line, 4-stroke, 6-cylinder Common Rail Direct Injection (CRDI) diesel engine designed to adhere to Euro IV emission standards. According to the manufacturer's specifications, the engine has a rated power output of 164 kW at 2500 rpm. Fig. 1 shows the schematic layout of the experimental setup, which provides a visual representation of the arrangement and connections, while key engine specifications are detailed in Table 2.

**Table 2**
Engine specification.

| Emission limits | Euro 4 |
|---|---|
| Intake and Exhaust valve stem diameters | 0.276 in x 0.276 in |
| Rated torque | 81.55 kg m @ 1000 rpm–1800 rpm |
| Rated power | 164 kW @ 2500 rpm |
| Injection system | Bosch high-pressure CR injection system |
| Bore x Stroke | 4.02 in x 4.72 in |
| CR | 17.2:1 |
| Displacement | 360 cu in |
| Firing order | 1-5-3-6-2-4 |
| Type | In-line, 4-S, 6-C, diesel engine |

The engine was equipped with a dynamometer, which played a crucial role in monitoring and adjusting critical parameters such as engine speed, brake power, and torque. This dynamometer ensured that the engine operated under controlled and consistent conditions throughout the experimentation. Temperature measurements were taken at several key locations, including the oil tank, water cooling system, intake manifold, and exhaust manifold, using K-type thermocouples. These thermocouples provided precise temperature data essential for analyzing the engine's performance and thermal behavior.

The fuel injection system employed was a Bosch common rail system, which was electronically controlled to maintain a fuel pressure of 138 MPa. The electronic injection controller, in conjunction with LabView software, was used to monitor and manage various parameters related to fuel injection, such as timing, quantity, and duration. This setup allowed for precise control and measurement of the fuel delivery process.

In-cylinder pressure was measured using a piezo-electric pressure transducer installed on the engine's cylinder head. To account for and minimize cycle-to-cycle variations, the average in-cylinder pressure was calculated from data collected over 100 consecutive cycles. Each cycle measurement covered an angular range of 0.23 degrees of crank angle. This approach ensured a high level of precision and reliability in the assessment of combustion dynamics within the engine.

#### 2.2.2. Engine operation

The experimental procedure for assessing the emission performance of a CRDI engine involves a series of carefully controlled steps to ensure accurate and reliable results. Initially, the engine was operated with pure diesel (D100) for a duration of 1380 s. This initial run was essential for establishing a dynamic equilibrium within the engine system. During this phase, stringent safety measures were implemented to prevent any potential hazards, and thorough inspections were conducted to check for any leaks of oil, fuel, or water, both before and during the experimental runs.

Once a steady-state condition was achieved, the engine was maintained at a consistent speed of 1700 rpm and operated under a 75 % load for the duration of the test. After this phase, any residual diesel fuel present in the fuel pipes, pump, and valves was carefully drained to avoid contamination in subsequent tests. The experimental procedure

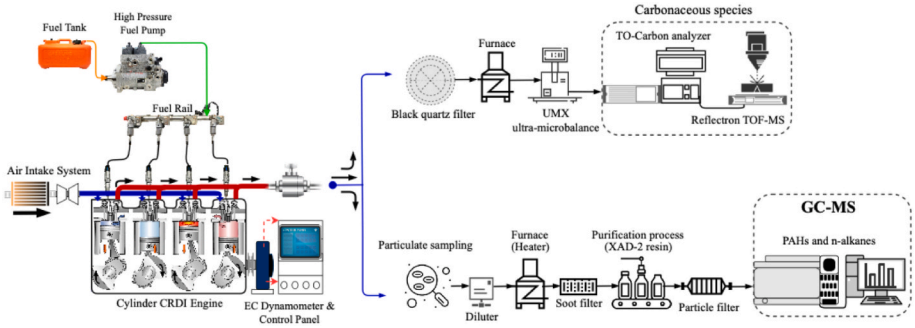


**Fig. 1.** Test engine and analytical setup.

was then repeated using six distinct fuel blends: L10 (10 % linseed oil and 90 % diesel), J10 (10 % jatropha oil and 90 % diesel), N10 (10 % neem oil and 90 % diesel), L30 (30 % linseed oil and 70 % diesel), J30 (30 % jatropha oil and 70 % diesel), and N30 (30 % neem oil and 70 % diesel).

Each testing cycle with the blended fuels lasted 600 s. During these cycles, comprehensive data was recorded to evaluate the engine's emissions when operating with different fuel compositions. Rigorous attention was given to maintaining consistent experimental conditions across all test runs to ensure the accuracy and reliability of the results. This methodical approach allowed for a thorough comparison of the effects of different fuel blends on engine emissions.

#### 2.2.3. Precision and measurement specifications for engine test instruments

Table 3 provides details on the accuracy, range, and uncertainty of various measurement instruments used in engine testing. The K-type thermocouple is employed for temperature measurements ranging from 0 to 1000 °C, with an accuracy of ±1 °C and an uncertainty of ±0.2 %. The crank angle encoder measures the crankshaft position within a full rotation of 0 to 360°, offering an accuracy of ±1° and an uncertainty of ±0.2 %. For pressure measurements, a transducer is used, capable of measuring pressures from 0 to 200 MPa with high precision, featuring an accuracy of ±0.001 MPa and an uncertainty of ±0.2 %. The load applied during testing is measured with a device that has an accuracy of ±0.1 N over a range of 0–10 kN, with an uncertainty of ±0.1 %. Lastly, engine speed is recorded with an accuracy of ±1 r/m, covering a range from 0 to 7500 r/m, with an uncertainty of ±0.2 %. These specifications ensure accurate and reliable data collection during engine testing.

### 2.3. Emissions

#### 2.3.1. EC and OC analyses

The method for analyzing elemental carbon (EC) and organic carbon (OC) in particulate matter involves several critical steps to ensure the accuracy and reliability of the data collected, as illustrated in Fig. 1. The process begins with the pre-treatment of blank quartz filters, which are heated at 550 °C for approximately 6 h in a muffle furnace. This high-temperature conditioning is necessary to eliminate any residual organic material or carbon that might otherwise contaminate the samples and interfere with the results. Once conditioned, the filters are stored under controlled conditions at 23 ± 1 °C to maintain their integrity and prevent any post-conditioning contamination.

Prior to sampling, the filters are carefully handled and weighed using a UMX ultra-microbalance. This highly sensitive balance is capable of detecting minute changes in mass, making it ideal for measuring the small amounts of particulate matter collected. The process of weighing is conducted with meticulous care to avoid introducing any contaminants. Specifically, direct contact with the calibration weight or the filters by fingers is strictly avoided, as even trace amounts of oils from the skin can skew the measurements.

After collecting particulate matter on the filters, the samples are subjected to thermal-optical analysis to quantify the EC and OC content. This analysis is performed using a thermal-optical carbon analyzer, which is coupled with a resonance-enhanced multiphoton ionization time-of-flight mass spectrometer (REMPI-ToF-MS). The thermal-optical method involves progressively heating the sample in an inert atmosphere to volatilize OC, followed by heating in an oxidizing atmosphere to combust EC. The evolution of carbon during these stages is monitored, allowing for the separation and quantification of OC and EC based on their distinct thermal and optical characteristics [25].

The REMPI-ToF-MS system provides additional analytical capabilities, enabling highly sensitive detection and characterization of the carbonaceous components. The laboratory ensures the accuracy and validity of the results by cross-referencing them with standard reference materials or known concentrations of OC and EC, providing a robust quality control measure. This comprehensive approach not only quantifies the total amount of carbon in particulate matter but also differentiates between its organic and elemental forms, offering valuable insights into the sources and nature of atmospheric particulate pollution [24].

**Table 3**
Accuracy, range, and uncertainty of measurement instruments for engine testing.

| Variable | Accuracy | Range | Uncertainty (%) |
|---|---|---|---|
| K-type thermocouple | ±1 °C | 0–1000 °C | ±0.2 |
| Crank angle encoder | ±1° | 0–360° | ±0.2 |
| Transducer | ±0.001 MPa | 0–200 MPa | ±0.2 |
| Load | ±0.1 N | 0–10 kN | ±0.1 |
| Speed | ±1 r/m | 0–7500 r/m | ±0.2 |

#### 2.3.2. n-Alkanes and PAHs analyses

In this study, samples of n-alkanes and particulate-phase PAHs are collected on glass-fiber filters, which are carefully prepared by pre-heating them in an oven at 475 °C for 4 h to eliminate potential contaminants. These preheated filters are stored in foil until used for sampling to prevent any contamination before analysis. The analysis is performed using a gas chromatography-mass spectrometer (GC-MS) equipped with an electron ionization source. The GC system includes a Phenomenex ZB-FFAP column (30 m × 320 μm × 0.25 μm), which is chosen for its ability to effectively separate the analytes. Helium serves as the carrier gas, facilitating the movement of compounds through the column. The GC column is temperature-controlled, allowing for precise separation of the target analytes, and is directly interfaced with the mass spectrometer's ion source for accurate detection.

In addition to the main GC-MS setup, a diluter is employed to manage the dilution range of the exhaust particulate samples. This is critical for ensuring that the concentrations of the analytes fall within the detection limits of the instrument. Pre-combusted Teflon® filters are used during this process to minimize the introduction of contaminants. The particulate matter collected on the filters is then processed using a separation unit that includes a high polyurethane form (PUF) sorbent tube. The PUF sorbent is particularly effective at trapping semi-volatile organic compounds, such as n-alkanes and PAHs, thus enhancing the sensitivity of the analysis. Quantification and monitoring of the analytes are conducted using the selected ion mode (SIM) of the mass spectrometer, which allows for the targeted detection of specific ions corresponding to the n-alkanes and PAHs. This selective approach increases the sensitivity and specificity of the analysis, enabling the accurate quantification of these compounds even at low concentrations. The method described is a modified version of the EPA TO-13A method. Details regarding the methodology can be found in the literature published [12,26,27].

### 2.4. Economic cost analysis

The economic analysis of biodiesel blends involves evaluating production costs, fuel efficiency, engine performance, and environmental benefits. Although utilizing biodiesel can significantly reduce greenhouse gas emissions and lower health costs associated with air pollution, initial investment in biodiesel production infrastructure and modifications to existing engines may pose economic challenges. To determine the most cost-effective blend, a comprehensive economic analysis is essential, taking into account agricultural productivity, engine modification costs, fuel efficiency, and the payback period for the initial investment.

To support this analysis, automated data acquisition systems were utilized to enhance testing efficiency by minimizing human error and enabling continuous data collection. Throughout these cycles, data was collected to assess engine performance with different fuel blends. Consistent experimental conditions were maintained to ensure accurate

and reliable results. This approach significantly contributed to the study, allowing for a thorough analysis of the economic and environmental performance of various biodiesel blends and offering valuable insights into their benefits and drawbacks. While the methods employed are reliable, there is room for improvement in measurement precision and data reliability. Future research could benefit from more advanced sensors and real-time data monitoring systems to further reduce uncertainties and improve the overall quality of the findings.

#### 2.4.1. Production cost per liter

The production cost per liter includes all expenses incurred in producing 1 L of biodiesel. It encompasses costs related to raw materials, processing, labor, overheads, and any other expenses associated with biodiesel production.

#### 2.4.2. Engine modification cost

Engine modification cost (EMC) refers to the expenses required to retrofit diesel engines to optimize them for the use of biodiesel blends. This may involve adjustments to fuel injection systems, engine components, or software upgrades to ensure compatibility and performance with biodiesel. It is calculated using the formula below:

$$EMC = (C_p + C_l) \quad \text{eqn. 1}$$

Where:

$C_p$ is the cost of the part

$C_l$ is the labor cost

#### 2.4.3. Payback period

The payback period calculates the time required for the savings generated using biodiesel blends to offset the initial investment in engine modifications. It is calculated using the formula below:

$$Payback\ Period\ (years) = \frac{EMC}{S_f} \quad \text{eqn. 2}$$

Annual savings $(S_f)$:

$$S_f = C_{diesel} \bullet F_{diesel} - C_{biodiesel} \bullet F_{diesel} \quad \text{eqn. 3}$$

$$F_{diesel} = \frac{D_a}{E_f} \quad \text{eqn. 4}$$

Where:

$C_{diesel}$ is the cost of diesel per liter.

$C_{biodiesel}$ is the cost of biodiesel per liter.

$F_{diesel}$ is the annual diesel consumption in liters.

$E_f$ is the fuel efficiency of diesel in km/liter.

$D_a$ is the annual distance traveled (km).

## 3. Results and discussion

### 3.1. Fuel properties and fatty acid contents

#### 3.1.1. Physical and chemical properties

For a biofuel to be classified as a good fuel, it must meet certain physicochemical properties standards, including viscosity, flash point, calorific value, pour point, density, and acid value. The fuel properties of diesel, neem, linseed, and jatropha biodiesels were compared and given in Table 4. The various properties show that the measured calorific value of the jatropha biodiesel is 35.7 MJ/kg. According to the literature, calorific value ranges between 35.5 and 38.0 MJ/kg of feedstock for rubber seed biodiesel [28,29]. On the other hand, the iodine value for neem biodiesel is low compared to linseed and jatropha biodiesel. A low iodine value gives better oxidative stability [12], meaning that linseed oil biodiesel is less reactive, more resistant to oxidation, and can be kept longer than neem biodiesel. Furthermore, linseed biodiesel might have a better cold flow property and can flow at lower temperatures compared to jatropha and neem biodiesel. This is reasonable because linseed biodiesel has a higher density and higher cetane value, which may result in a shorter ignition delay and a better cold flow property compared to jatropha and neem biodiesel.

**Table 4**
Comparisons of physical and chemical properties of diesel, neem, linseed, and jatropha biodiesel.

| Properties | Test method | Diesel | Neem | Linseed | Jatropha |
|---|---|---|---|---|---|
| Density (kg/m$^3$) | D 1298 | 837 | 857 | 883 | 881 |
| Calorific value (MJ/kg) | D 240 | 43.80 | 42.20 | 40.51 | 35.7 |
| Cetane value | D 613 | 54.40 | 55.40 | 56 | 53.34 |
| Iodine value (g/100g) | – | – | 89.57 | 169 | 102 |
| Kinematic viscosity at 40 °C (cSt) | D 445 | 2.51 | 4.42 | 4.5 | 4.84 |
| Flash point (°C) | D 93 | 59.30 | 164 | 173 | 163 |
| Pour point (°C) | D97 | −16 | 2 | −9 | −6 |
| Cloud point (°C) | D2500 | −1 | −3 | −1 | 9 |

The kinematic viscosities of neem, jatropha, and linseed methyl esters are 4.42, 4.84, and 4.50 mm$^2$/s, respectively. This variation in the viscosity was generally due to the different nature of the parent oil and the product of the yield of methyl esters, given that it is quite impossible to have similar biodiesel from different parent oils. The result showed that the neem oil methyl ester has the lowest kinematic viscosity, followed by the linseed and jatropha oil biodiesel. When biodiesel is combined with low and high-sulfur diesel, along with varying proportions of diesel, the viscosity of the resulting blends also fluctuates accordingly. The viscosity of blends experiences an upward trend with the rise in the percentage of low-sulfur diesel, attributed to the elongation of hydrocarbon chain lengths within low-sulfur diesel [30]. Conversely, an increase in the proportion of high-sulfur diesel in the blend leads to a reduction in viscosity [31]. This phenomenon can be attributed to the sulfur content promoting the formation of oxides smaller in size than nitrogen. Consequently, this results in shorter chain lengths and enhances the fluidity of the blends, facilitating easier flow through the fuel lines.

#### 3.1.2. Chemical composition analysis

Table 5 presents a comparative analysis of the fatty acid composition found in neem, linseed, and jatropha biodiesel. The proportions of saturated, monounsaturated, and polyunsaturated fatty acids in neem, jatropha, and linseed biodiesel differ significantly. The most abundant type in neem and jatropha biodiesel is monounsaturated fatty acids, whereas, in linseed biodiesel, it is polyunsaturated fatty acids. This is somewhat related to the findings in section 3.1.1, as the different types of fatty acids in each biodiesel may directly contribute to the varied viscosity and density results obtained [12]. Given neem oil's substantial oleic acid content, the resulting fatty acid methyl esters are expected to exhibit desirable fuel properties, particularly regarding cetane number and viscosity. This observation aligns with consistent findings across various studies [26,32]. Additionally, the present study reveals that Jatropha oil exhibits a favorable fatty acid profile, positioning it as a promising source for biodiesel production compared to other commonly used vegetable oils [33]. This preference likely stems from the

**Table 5**
Comparison of fatty acid of neem, linseed, and jatropha biodiesels.

| Biodiesel | Fatty acid composition (%) | | | | | |
|---|---|---|---|---|---|---|
| | Palmitic C16:0 | Stearic C18:0 | Oleic C18:1 | Linoleic C18:2 | Linolenic C18:3 | Others |
| Neem | 13.18 | 14.91 | 48.72 | 15.38 | 0.25 | 7.56 |
| Linseed | 5.73 | 3.51 | 14.09 | 15.62 | 60.18 | 0.87 |
| Jatropha | 13.84 | 6.51 | 37.96 | 39.68 | – | 2.01 |

predominant presence of C18 fatty acid chains, known for imparting superior oxidation stability and improved cold flow properties compared to C16 fatty acid chains [13,34].

### 3.2. Effect of blended fuels on VOC emission species

#### 3.2.1. Effect of N10 and N30 blended fuels on VOC emission species

Fig. 2 represents the composition of particulate organic matter for total VOCs. A total of 27 VOCs were identified and quantified in the engine exhaust, which includes PAHs, alkanes, alkenes, and halogenated hydrocarbons. Among the pollutants mentioned, halogenated hydrocarbons are often considered more hazardous due to their toxicological and environmental effects [35]. However, other pollutants like PAHs and unburned aromatic hydrocarbons also pose significant risks due to their carcinogenic and mutagenic properties, which could potentially cause cancer in humans and change the genetic material within a person's cell, causing mutations [24]. This is particularly concerning given that, according to the World Health Organization, around 4.2 million deaths yearly occur due to outdoor air pollution exposure [36]. Evidence suggests that these deaths are primarily associated with exposure to particles, depending on the specific compounds involved and the circumstances of exposure [24].

In this study, emissions of the higher molecular weight PAHs are lower with neem biodiesel blends, and there is a marked decrease in emissions as the blend level is increased from N10 to N30. High molecular weight PAHs are of more significant concern because of their higher carcinogenic potential [37], which led to regulations to limit their concentration. The percentage reduction in total PAH emission for N10 and N30 blend fuels is 10.7 % and 38.4 %, respectively, compared to that for D100. This decrease in PAH levels could potentially mitigate the risk of cancer and alleviate eye irritation caused by allergens in animals and humans [26].

Alkanes are mainly formed during incomplete fuel combustion. They are classified into three groups: volatile (C4-C10), semi-volatile (C11-C15), and non-volatile paraffin (C16 upwards). Fig. 2 shows that the total N30 blend results in a reduction of the three groups compared with the N10 blend. This aligns with the observed trend in specific fuel consumption, as the engine burns more volatile alkanes, resulting in a lower amount being emitted in the exhaust [38]. As shown in Fig. 2, the N10 fuel emitted 17 % less formaldehyde than the D100 tests, and the N30 blend emitted 76 % less than the diesel. Similar trends were also obtained with trichlorofluoromethane, 2-methylbutane, naphthalene, and acetaldehyde for the N30 fuel, which emitted fewer toxins than all the test fuels. This presents a promising outlook for human health, as outlined in the introduction, due to the reduced emission of toxic compounds.

Compared to D100 fuel, N10 fuel shows reductions of 1.1 %, 2.3 %, 3.7 %, and 2.6 % for toluene, p-xylene, ethylbenzene, and o-xylene, respectively. Similarly, N30 fuel demonstrates reductions of 3.2 %, 2.3 %, 5.8 %, and 6.8 % for the same compounds. This finding is slightly lower than those in the previous research by Refs. [39,40]. This phenomenon may be attributed to improved atomization during injection, which results in more efficient combustion and fewer incomplete combustion products, including PAHs [12]. Additionally, the higher oxygen content may promote better fuel combustion, leading to reduced emissions of incomplete combustion products [41], which are major contributors to most of the VOCs found in the raw exhaust gas.

#### 3.2.2. Effect of J10 and J30 blended fuels on VOC emission species

As shown in Fig. 2, unburned aromatic compounds and PAHs increased in J10 emissions, which are considered a disadvantage of using Jatropha blend fuel in comparison to other blend fuels. The increase in VOC species from J10 and D100 may be attributed to the high aromatic and low cetane contents [42]. However, it is evident that the increase in jatropha biodiesel in the blend results in higher VOC reduction efficiencies. The lower emission for the J30 might be due to a lower amount of monounsaturated compounds present, which resulted in better combustion and less formation of VOCs.

Besides, with the use of J10 fuel, emissions of primary hydrocarbons such as nonadecane, trichlorofluoromethane, triacontane, and 1,2-dichloroethane decreased. This improvement can be attributed to enhanced volatility and combustion efficiency, leading to reduced emissions of heavier hydrocarbons in the exhaust [12]. Although, certain compounds such as naphthalene, eicosane, and triacontane exhibited higher emissions peaks.

J10 fuel combustion produced total PAH emissions of 0.956 mg/kWh, higher than the 0.886 mg/kWh emitted by D100, whereas J30 fuel exhibited even lower emissions at 0.742 mg/kWh. With D100 fuel, the PAH emission levels followed the order of benzo(a)pyrene (BaP) > dibenz[a,h]anthracene > 3OH-BaP > toluene. When using J10 fuel, both BaP and 3OH-BaP emission levels increase, whereas, with J30 fuel, PAH isomer emission levels significantly decrease. It was also observed that dibenzo[a,h]anthracene, indeno(1,2,3-cd)pyrene, BaP, and benzo(ghi)perylene emissions exhibited a notable increase when J10 fuel was combusted compared to all tested fuels. This increase can be attributed to the composition and properties of the J10 fuel blend, which may contain higher concentrations of aromatic hydrocarbons. Aromatics tend to produce more PAHs during combustion due to their complex

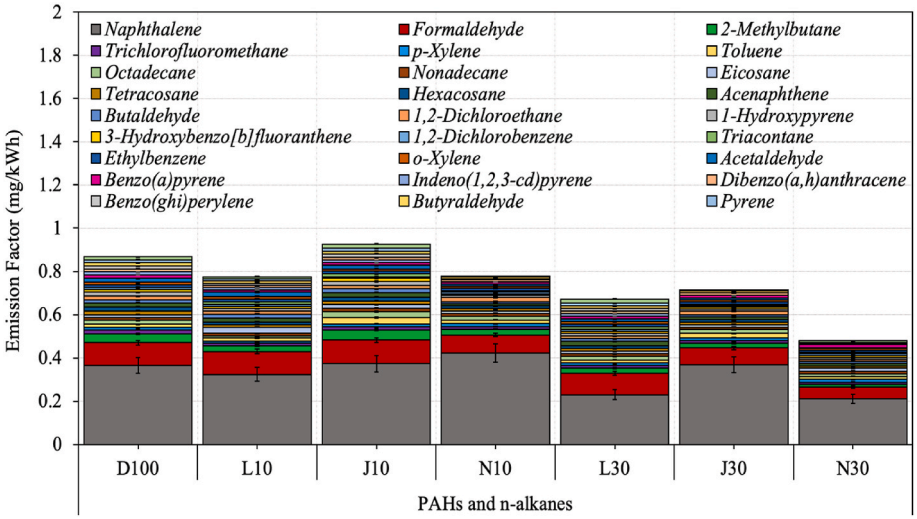


**Fig. 2.** Effect of various blend fuels on VOCs emission species.

molecular structure [22]. Additionally, incomplete combustion or sub-optimal combustion conditions, such as lower combustion temperatures or poor air-fuel mixing, can lead to the formation and emission of these PAHs. These PAH emissions are concerning because they are known to be hazardous air pollutants with potential carcinogenic and mutagenic effects [43]. Specifically, compounds like BaP and dibenzo[a,h]anthracene are classified as probable human carcinogens, posing significant environmental and public health concerns [44].

### 3.2.3. Effect of L10 and L30 blended fuels on VOC emission species

The proportion of individual alkanes in total alkanes depends on the number of carbon atoms. Hence, eicosane, hexacosane, and tetracosane are major alkanes in all cases, as shown in Fig. 2. These are highly branched alkanes, and their presence is due to the CRDI-type engine used [24,41]. These alkanes are also found in advanced diesel engine, vegetable oils, and their methyl/ethyl esters [26]. They will take some time to burn and may cause smoke. As observed, L10 fuel causes faster and better combustion and high PM, but engine deposits remain unclear as the long alkyl chain alkanes have not been reduced significantly compared to L30, which is the best option compared to D100.

Typically, diesel engines emit higher levels of naphthalene and acenaphthene due to less complete combustion processes. However, the result shows that the naphthalene emissions were 0.324 mg/kWh for L10 and 0.229 mg/kWh for L30, slightly lower than D100, with a percentage decrease of 11.24 % and 37.14 %, respectively. These reductions are due to the higher cetane number and oxygen content in the biodiesel blend, which enhances combustion completeness [33]. The L30 blend demonstrates a substantial decrease in emissions, often reducing heavier PAH levels, such as indeno(1,2,3-cd)pyrene, dibenzo [a,h]anthracene, benzo[ghi]perylene, and BaP, by more than 21.3 % compared to D100, while L10 achieves reductions of 13.4 %. This reduction in emissions can be attributed to several factors, including the lower aromatic content in these blends, which results in fewer precursors available for PAH formation during combustion [24]. Additionally, the inclusion of lighter components in the blends can enhance combustion efficiency, promoting more complete combustion and thereby reducing the formation of PAHs [23,26]. The presence of oxygenates in the blends may also improve the oxidation process, further lowering the emission of these harmful compounds.

The emissions of p-xylene, toluene, ethylbenzene, and o-xylene showed a clear decline as the proportion of biodiesel in the fuel increased. The D100 fuel exhibits the highest emission levels of these compounds, primarily due to its lower combustion efficiency and lack of oxygen content. In contrast, L10 reduces these emissions by approximately 17.8 %, as the higher oxygen content in biodiesel promotes more complete combustion. However, the reduction becomes even more pronounced with L30, reaching up to 34.9 %. This reduction can be attributed to the increased oxygen content in biodiesel, which enhances the combustion process and reduces the formation of incomplete combustion byproducts [20,45]. These emissions, if not controlled, can contribute to air pollution and have adverse health effects. VOCs such as p-xylene, toluene, ethylbenzene, and o-xylene are known to be harmful, with the potential to cause respiratory issues, headaches, and other health problems [46]. Long-term exposure to these compounds can also lead to more severe conditions, including liver and kidney damage and an increased risk of cancer [47]. Furthermore, specific PAH derivatives, such as 1-hydroxypyrene and 3-hydroxybenzo[b]fluoranthene, show significant emission reductions. These reductions are more pronounced with L30, achieving up to 12.7 %, compared to 6.2 % with L10, due to the higher biodiesel content enhancing combustion quality.

## 3.3. PM-bound carbon emissions

### 3.3.1. Effect of N10 and N30 blended fuels on EC and OC emissions

As shown in Fig. 3, the EC emissions decreased from 0.0322 g/kWh for D100 to 0.0297 g/kWh for J10. Similarly, OC emissions dropped from 0.0309 g/kWh for D100 to 0.0282 g/kWh for J10, indicating a reduction of 9 %. The J30 blend exhibited an even greater reduction in emissions compared to both the D100 and J10 blends. EC emissions decreased to 0.0264 g/kWh, marking a reduction of 18 % from D100 levels, while OC emissions dropped to 0.0247 g/kWh, showcasing a reduction of approximately 20 % compared to D100. This decrease in emissions with increasing blend ratio suggests a dose-dependent relationship between biodiesel concentration and emissions reduction. As the proportion of biodiesel in the blend increases, the oxygen content rises accordingly [48], promoting more efficient combustion and lowering EC and OC emissions. However, it's essential to consider the diminishing returns phenomenon; beyond a certain blend percentage, the incremental benefits of increasing biodiesel concentration may become marginal.

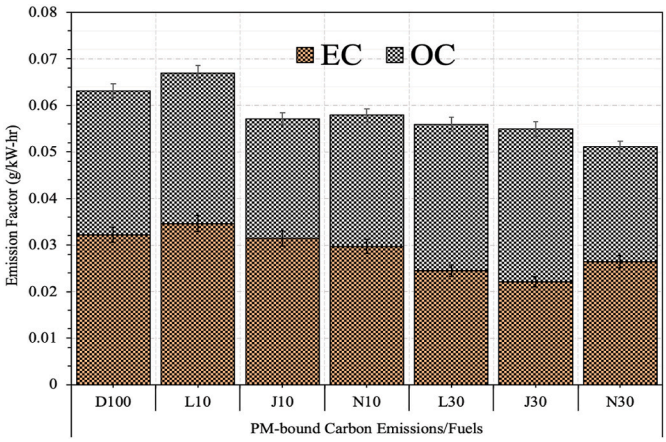


**Fig. 3.** Effect of various blend fuels on particle-bound carbon emissions.

The observed decrease in OC and EC emissions can be attributed to several factors. Firstly, neem biodiesel possesses lower sulfur content compared to D100 fuel, thereby reducing the formation of sulfur-derived particulate matter [49]. Additionally, neem biodiesel has higher oxygen content, facilitating more complete combustion and minimizing the formation of carbonaceous particles [50]. Moreover, biodiesel blends typically have lower aromatic and polyaromatic hydrocarbon content compared to D100, further leading to reduced soot formation and subsequently lowering EC emissions. This is consistent with previous studies that have demonstrated the potential of fuel alternatives to decrease particulate emissions, particularly EC and OC, due to their oxygen content and superior combustion characteristics [12,51].

Moreover, the molecular structure of neem biodiesel, characterized by its long-chain fatty acid methyl esters, influences the combustion process by promoting better atomization and mixing with air, resulting in fewer carbonaceous particulates during combustion. Furthermore, neem biodiesel has inherent lubricating properties that can potentially mitigate wear and tear on engine components, thereby improving combustion efficiency and reducing the generation of particulate matter.

### 3.3.2. Effect of J10 and J30 blended fuels on EC and OC emissions

As shown in Fig. 3, the J30 blend demonstrated the most pronounced reduction in EC emissions, with a noteworthy decrease from 0.0322 g/kWh for D100 to 0.0221 g/kWh, indicating a substantial mitigation effect on particulate matter emissions compared to both D100 and J10. This reduction could be attributed to the higher oxygen content and lower carbon-to-hydrogen ratio of biodiesel [48], which promotes more complete combustion and, subsequently, lower EC emissions.

Interestingly, the impact on OC emissions exhibited a contrasting trend. While J30 showed a slight increase in OC emissions compared to D100, rising from 0.0309 g/kWh to 0.0328 g/kWh, the J10 blend demonstrated a notable reduction in OC emissions, dropping to 0.0257 g/kWh. Despite the reduction in EC, this rise in OC emissions could be

due to the higher viscosity and lower volatility of J30, which might lead to incomplete combustion and higher unburned hydrocarbon formation [24].

However, the increase in OC emissions with the J30 blend highlights the complexity of fuel formulation and combustion dynamics. Therefore, optimizing the blend ratio and improving engine calibration for higher biodiesel content could be crucial steps toward achieving a balanced reduction in both EC and OC emissions. Additionally, the lower OC emissions observed in the J10 blend could be attributed to the improved oxygenation effect and more efficient combustion achieved with the addition of Jatropha biodiesel, leading to a more complete oxidation of organic compounds [33].

#### 3.3.3. Effect of L10 and L30 blended fuels on EC and OC emissions

EC is more optically absorptive than OC and poses a significant risk to public health for both $PM_{2.5}$ and $PM_{10}$ due to its tightly controlled measurement techniques and strong association with adverse health effects [52]. OC is less absorptive than EC and consists of various organic compounds, contributing to its health impacts. EC and OC in the complex mixture of diesel exhaust particles are believed to contribute to the risk of lung cancer [53]. From the figure (Fig. 3), it is seen that there is substantial variation in each OC and EC result. For the L10 blend, EC emissions showed a marginal increase of 2 % compared to D100. This slight increase might be due to the lower combustion temperatures associated with linseed biodiesel, which inhibit the complete oxidation of carbon into $CO_2$, leaving more elemental carbon as soot. Conversely, the L30 blend demonstrated a more substantial decrease in EC emissions, with a reduction of 31.43 %. This reduction can be explained by the better combustion characteristics of linseed biodiesel, which promote more complete combustion and thus lower the formation of soot and EC [54]. This observation also indicates a potential nonlinear relationship between biodiesel blend ratios and EC emissions, where higher blend ratios may not necessarily lead to proportionally higher EC emissions.

The OC emissions for D100 were recorded at 0.0309 g/kWh, which is slightly lower compared to L10 and L30, with their values being 0.0324 g/kWh and 0.0314 g/kWh, respectively. However, the extent of EC reduction with the L30 blend was less pronounced than that of OC, indicating that the blend improves overall combustion. Reducing EC may require a higher biodiesel content. This suggests that while L30 may offer advantages regarding EC emissions reduction, its effect on OC emissions may not be as significant.

## 4. Economic impact analysis

### 4.1. Cost-benefit analysis

Table 6 compares the production cost, engine modification cost, fuel efficiency, annual savings, and payback period for various fuel blends. The J10 blend offers a production cost of $0.93 per liter and a one-time engine modification cost of $310. With a commendable fuel efficiency of 18.1 km per liter, the annual savings amount to $270, derived from the difference between D100 fuel costs ($1.20 per liter) and that of the J10 blend. Consequently, the payback period for the engine modification investment is 1.15 years. Similarly, the J30 blend, with a lower production cost of $0.90 per liter but a slightly higher engine modification cost of $320, demonstrates an even shorter payback period of about 1.07 years, owing to its improved fuel efficiency of 18.5 km/l.

**Table 6**
Comparative analysis of production costs, engine modification costs, fuel efficiencies, annual savings, and payback periods for various fuel blends.

| Blend | Production Cost ($/liter) | Engine Modification Cost ($) | Fuel Efficiency (km/l) | Annual Savings ($) | Payback Period (years) |
|---|---|---|---|---|---|
| J10 | 0.93 | 310 | 18.1 | 270 | 1.15 |
| J30 | 0.90 | 320 | 18.5 | 300 | 1.07 |
| N10 | 0.98 | 315 | 16.7 | 220 | 1.43 |
| N30 | 1.00 | 305 | 17.2 | 200 | 1.53 |
| L10 | 1.05 | 300 | 16.9 | 150 | 2.00 |
| L30 | 1.09 | 295 | 15.9 | 110 | 2.68 |

However, the Neem blends, N10 and N30, exhibit higher production costs than the Jatropha blends, respectively, at $0.98 and $1.00 per liter. Furthermore, their engine modification costs are slightly lower at $315 and $305. With fuel efficiencies of 16.7 and 17.2 km per liter, respectively, these blends generate annual savings of $220 and $200. As a result, the payback periods for the N10 and N30 blends are approximately 1.43 and 1.53 years, respectively, indicating slightly longer but still favorable returns on investment.

In contrast, the Linseed blends, L10 and L30, exhibit the highest production costs among the blends, at $1.05 and $1.09 per liter, respectively. Their engine modification costs are comparable to the Neem blends at $300 and $295. Despite a fuel efficiency advantage of 16.9 km per liter for the L10 blend and a lower efficiency of 15.9 km/l for the L30 blend, their annual savings amount to $150 and $110, respectively. Consequently, the payback periods for the L10 and L30 blends are 2.00 and 2.68 years, respectively, indicating slower investment returns than the other blends.

### 4.2. Discussion

The analysis reveals distinct trends across the different biodiesel blends, reflecting variations in production costs, engine modification expenses, fuel efficiency, annual savings, and payback periods. One noticeable trend is the inverse relationship between production costs and payback periods. Blends with lower production costs, such as the Jatropha blends, tend to exhibit shorter payback periods, indicating quicker returns on investment in engine modifications. Conversely, blends with higher production costs, such as the Linseed blends, generally entail longer payback periods, suggesting a slower recoupment of the initial investment.

Moreover, a positive correlation between fuel efficiency and annual savings is evident, contributing to shorter payback periods. Blends with higher fuel efficiency, like the J30 blend, lead to greater annual savings, thus accelerating the payback process. This shows the importance of fuel efficiency in optimizing the economic viability of biodiesel blends. Additionally, variations in engine modification costs influence the overall investment required and subsequently impact the payback period. For instance, while the Neem blends have slightly lower engine modification costs compared to the Jatropha blends, their higher production costs result in slightly longer payback periods.

Furthermore, the trends highlight the trade-offs between economic considerations and environmental benefits. While blends like Jatropha and Neem offer favorable economic returns with relatively shorter payback periods, they also contribute to reduced emissions and promote sustainable fuel alternatives. On the other hand, blends with longer payback periods, such as Linseed, may require additional incentives or policy support to enhance their economic attractiveness despite their environmental advantages.

## 5. Conclusion and Recommendations

This study provides a thorough analysis of biodiesel blends derived from neem, jatropha, and linseed oils, focusing on their production, properties, emissions, and economic impact on diesel engine. Our key findings are as follows.

1. Neem biodiesel exhibited the lowest viscosity, indicating improved flow characteristics, while linseed biodiesel had a higher cetane value and density, with promising cold flow properties. Jatropha biodiesel demonstrated a favorable fatty acid profile, high calorific

value, and superior oxidation stability, making it a competitive option among biodiesel sources.

2. Neem biodiesel blends significantly reduced high molecular weight PAHs, mitigating health risks associated with carcinogenic compounds. Jatropha biodiesel blends also led to substantial reductions in formaldehyde and naphthalene, enhancing air quality and reducing respiratory disease risks. The emissions analysis showed that higher biodiesel content generally led to reduced EC and OC emissions, indicating improved combustion efficiency. Notably, the J30 jatropha blend achieved the greatest reduction in EC emissions, though it slightly increased OC emissions, suggesting the need for optimized engine calibration.
3. The economic evaluation revealed that biodiesel blends like jatropha and neem have shorter payback periods due to lower production costs and significant savings on engine modifications and fuel efficiency. Conversely, linseed biodiesel, with its higher production costs, has a longer payback period but still contributes positively to emissions reduction and sustainability.

Our analysis highlights that not all biodiesel blends offer uniform environmental benefits. This underscores the need for a tailored approach in biofuel policies rather than a one-size-fits-all strategy. Detailed assessments of each biodiesel type, considering raw materials, geographical factors, and extraction techniques, are essential. Policymakers should promote blends with consistent environmental benefits and incentivize research and development to improve extraction techniques and optimize blends. Furthermore, modern diesel engines with advanced technologies may perform differently with biodiesel compared to older models, suggesting that ongoing research in engine technologies is crucial to maximizing biodiesel benefits.

## CRediT authorship contribution statement

**Abdulfatah Abdu Yusuf:** Writing – original draft, Validation, Methodology, Investigation, Conceptualization. **Ibham Veza:** Visualization, Validation, Formal analysis, Data curation. **Zubeda Ukundimana:** Validation, Formal analysis, Data curation. **Adolphus Nippae:** Visualization, Validation, Formal analysis, Data curation. **Charles Asumana:** Visualization, Formal analysis, Data curation. **Eric Kay Jebboe:** Visualization, Validation, Formal analysis, Data curation. **M.A. Mujtaba:** Visualization, Validation, Formal analysis, Data curation. **Islam Md Rizwanul Fattah:** Validation, Formal analysis, Data curation. **Manzoore Elahi M. Soudagar:** Validation, Formal analysis, Data curation.

## Declaration of competing interest

The authors declare that they have no known competing financial interests or personal relationships that could have appeared to influence the work reported in this paper.

## Data availability

Data will be made available on request.

## References


[1] V.J. Reddy, N.P. Hariram, R. Maity, M.F. Ghazali, S. Kumarasamy, Sustainable Vehicles for decarbonizing the transport sector: a comparison of biofuel, electric, fuel cell and solar-powered vehicles, World Electr. Veh. J. 15 (2024) 93, https://doi.org/10.3390/wevj15030093.

[2] R. Garg, R. Sabouni, M. Ahmadipour, From waste to fuel: challenging aspects in sustainable biodiesel production from lignocellulosic biomass feedstocks and role of metal organic framework as innovative heterogeneous catalysts, Ind. Crops Prod. 206 (2023) 117554, https://doi.org/10.1016/j.indcrop.2023.117554.

[3] A. Arumugam, V. Ponnusami, Biodiesel production from Calophyllum inophyllum oil a potential non-edible feedstock: an overview, Renew. Energy 131 (2019) 459–471, https://doi.org/10.1016/j.renene.2018.07.059.

[4] A.A. Yusuf, V. Karthickeyan, S.S. Nura, A.H. Shu'ibu, A.A. Farooq, F.L. Inambao, Data set on performance and relative exhaust emission (REE) characteristics of fish oil ethyl ester with fuel preheating in diesel engine, Data Br 29 (2020) 105237, https://doi.org/10.1016/j.dib.2020.105237.

[5] A. Haq, M. Laiq Ur Rehman, Q. ul A. Rana, A. Khan, W. Sajjad, H. Khan, S. Khan, A. A. Shah, F. Hasan, S. Ahmed, A. Islam, M. Badshah, T.A. Shah, T.M. Dawoud, M. Bourhia, Production, optimization, and physicochemical characterization of biodiesel from seed oil of indigenously grown Jatropha curcas, Front. Energy Res. 11 (2023), https://doi.org/10.3389/fenrg.2023.1225988.

[6] H.A. Debella, V.R. Ancha, S.M. Atnaw, Production, optimization, and characterization of Ethiopian variant Prosopis juliflora based biodiesel, Heliyon 9 (2023) e15721, https://doi.org/10.1016/j.heliyon.2023.e15721.

[7] P. Puspitasari, D. Dwi Pramono, D. Nur Fiansyah, A. Ayu Permanasari, N. Mufti, J. Abd Razak, Biodiesel production from waste cooking oil using calcium oxide derived from scallop shell waste, Clean Energy 8 (2024) 113–126, https://doi.org/10.1093/ce/zkae005.

[8] D. Abooali, R. Soleimani, S. Gholamreza-Ravi, Characterization of physico-chemical properties of biodiesel components using smart data mining approaches, Fuel 266 (2020) 117075, https://doi.org/10.1016/j.fuel.2020.117075.

[9] H. Çamur, E. Alassi, Physicochemical properties enhancement of biodiesel synthesis from various feedstocks of waste/residential vegetable oils and palm oil, Energies 14 (2021) 4928, https://doi.org/10.3390/en14164928.

[10] G. Singh, C. Jeyaseelan, K.K. Bandyopadhyay, D. Paul, Comparative analysis of biodiesel produced by acidic transesterification of lipid extracted from oleaginous yeast Rhodosporidium toruloides, 3 Biotech. 8 (2018) 434, https://doi.org/10.1007/s13205-018-1467-9.

[11] F. Binhweel, M. Bahadi, H. Pyar, A. Alsaedi, S. Hossain, M.I. Ahmad, A comparative review of some physicochemical properties of biodiesels synthesized from different generations of vegetative oils, J. Phys. Conf. Ser. 1900 (2021) 012009, https://doi.org/10.1088/1742-6596/1900/1/012009.

[12] A.A. Yusuf, D.A. Yusuf, Z. Jie, T.Y. Bello, M. Tambaya, B. Abdullahi, I. A. Muhammed-Dabo, I. Yahuza, H. Dandakouta, Influence of waste oil-biodiesel on toxic pollutants from marine engine coupled with emission reduction measures at various loads, Atmos. Pollut. Res. 13 (2022) 101258, https://doi.org/10.1016/j.apr.2021.101258.

[13] M.O. Kareem, G.D.J.G. Pena, A. Raj, M.M. Alrefaai, S. Stephen, T. Anjana, Effects of neem oil-derived biodiesel addition to diesel on the reactivity and characteristics of combustion-generated soot, Energy Fuel. 31 (2017) 10822–10832, https://doi.org/10.1021/acs.energyfuels.7b01053.

[14] W.C. Ulakpa, R.O.E. Ulakpa, M.C. Egwunyenga, T.C. Egbosiuba, Transesterification of non-edible oil and effects of process parameters on biodiesel yield, Clean, Waste Syst. 3 (2022) 100047, https://doi.org/10.1016/j.clwas.2022.100047.

[15] A.J. Folayan, A. Dosunmu, A.B. Oriji, Synthesis and characterization of polyvalent high-performance synthetic base oil for drilling operations in recalcitrant and unconventional oil and gas reservoirs, South African J. Chem. Eng. 46 (2023) 143–164, https://doi.org/10.1016/j.sajce.2023.08.001.

[16] J.V.L. Ruatpuia, G. Halder, M. Vanlalchhandama, F. Lalsangpuii, R. Boddula, N. Al-Qahtani, S. Niju, T. Mathimani, S.L. Rokhum, Jatropha curcas oil a potential feedstock for biodiesel production: a critical review, Fuel 370 (2024) 131829, https://doi.org/10.1016/j.fuel.2024.131829.

[17] S. Hassan, A. Taghizadeh-alisaraei, B. Ghobadian, A. Abbaszadeh-mayvan, Performance and emission characteristics of a CI engine fuelled with carbon nanotubes and diesel-biodiesel blends, Renew. Energy 111 (2017) 201–213, https://doi.org/10.1016/j.renene.2017.04.013.

[18] V. Dhana Raju, J.N. Nair, H. Venu, L. Subramani, M.E. Manzoore, M.A. Mujtaba, T. M.Y. Khan, K.A. Ismail, A. Elfasakhany, A.A. Yusuf, B.A. Mohamed, I.M.R. Fattah, Combined assessment of injection timing and exhaust gas recirculation strategy on the performance, emission and combustion characteristics of algae biodiesel powered diesel engine, Energy Sources, Part A Recover. Util. Environ. Eff. 44 (2022) 8554–8571, https://doi.org/10.1080/15567036.2022.2123068.

[19] A.A. Yusuf, H. Yahyah, A.A. Farooq, K.A. Buyondo, P.W. Olupot, S.S. Nura, T. Sanni, T. Hannington, Z. Ukundimana, A.S. Hassan, M.M. Mundu, S.S. Samede, Y.A. Makeri, M.D. Selvam, Characteristics of ultrafine particle emission from light-vehicle engine at city transport-speed using after-treatment device fueled with n-butanol-hydrogen blend, Case Stud. Chem. Environ. Eng. 3 (2021) 100085, https://doi.org/10.1016/j.cscee.2021.100085.

[20] A.A. Yusuf, F.L. Inambao, A.A. Farooq, Impact of n-butanol-gasoline-hydrogen blends on combustion reactivity, performance and tailpipe emissions using TGDI engine parameters variation, Sustain. Energy Technol. Assessments 40 (2020) 100773, https://doi.org/10.1016/j.seta.2020.100773.

[21] I. Veza, Irianto, A. Tuan Hoang, A.A. Yusuf, S.G. Herawan, M.E.M. Soudagar, O. D. Samuel, M.F.M. Said, A.S. Silitonga, Effects of Acetone-Butanol-Ethanol (ABE) addition on HCCI-DI engine performance, combustion and emission, Fuel 333 (2023) 126377, https://doi.org/10.1016/j.fuel.2022.126377.

[22] G. Venkatraman, N. Giribabu, P.S. Mohan, B. Muttiah, V.K. Govindarajan, M. Alagiri, P.S. Abdul Rahman, S.A. Karsani, Environmental impact and human health effects of polycyclic aromatic hydrocarbons and remedial strategies: a detailed review, Chemosphere 351 (2024) 141227, https://doi.org/10.1016/j.chemosphere.2024.141227.

[23] A.A. Yusuf, J.D. Ampah, I. Veza, A.E. Atabani, A.T. Hoang, A. Nippae, M.T. Powoe, S. Afrane, D.A. Yusuf, I. Yahuza, Investigating the influence of plastic waste oils and acetone blends on diesel engine combustion, pollutants, morphological and size particles: dehalogenation and catalytic pyrolysis of plastic waste, Energy Convers. Manag. 291 (2023) 117312, https://doi.org/10.1016/j.enconman.2023.117312.

[24] A.A. Yusuf, J. Dankwa Ampah, M.E.M. Soudagar, I. Veza, U. Kingsley, S. Afrane, C. Jin, H. Liu, A. Elfasakhany, K.A. Buyondo, Effects of hybrid nanoparticle additives in n-butanol/waste plastic oil/diesel blends on combustion, particulate and gaseous emissions from diesel engine evaluated with entropy-weighted PROMETHEE II and TOPSIS: environmental and health risks of plastic wa, Energy Convers. Manag. 264 (2022) 115758, https://doi.org/10.1016/j.enconman.2022.115758.
[25] Z.H. Zhang, R. Balasubramanian, Effects of cerium oxide and ferrocene nanoparticles addition as fuel-borne catalysts on diesel engine particulate emissions: environmental and health implications, Environ. Sci. Technol. 51 (2017) 4248–4258, https://doi.org/10.1021/acs.est.7b00920.
[26] A.A. Yusuf, F.L. Inambao, J.D. Ampah, Evaluation of biodiesel on speciated PM2.5, organic compound, ultrafine particle and gaseous emissions from a low-speed EPA Tier II marine diesel engine coupled with DPF, DEP and SCR filter at various loads, Energy 239 (2022) 121837, https://doi.org/10.1016/j.energy.2021.121837.
[27] U.S. EPA, Compendium of methods for the determination of toxic organic compounds in ambient air, compendium method TO-13a: determination of polycyclic aromatic hydrocarbons (PAHs) in ambient air using gas chromatography/mass spectrometry (GC/MS), Cent. Environ. Res. Inf. Off. Res. Dev. U.S. Environ. Prot. Agency Cincinnati, OH 45268. II (1999) 78.
[28] M. Morshed, K. Ferdous, M.R. Khan, M.S.I. Mazumder, M.A. Islam, M.T. Uddin, Rubber seed oil as a potential source for biodiesel production in Bangladesh, Fuel 90 (2011) 2981–2986, https://doi.org/10.1016/j.fuel.2011.05.020.
[29] V.E. Geo, A. Sonthalia, G. Nagarajan, B. Nagalingam, Studies on performance, combustion and emission of a single cylinder diesel engine fuelled with rubber seed oil and its biodiesel along with ethanol as injected fuel, Fuel 209 (2017) 733–741, https://doi.org/10.1016/j.fuel.2017.08.036.
[30] G. Knothe, K.R. Steidley, Kinematic viscosity of biodiesel fuel components and related compounds. Influence of compound structure and comparison to petrodiesel fuel components, Fuel 84 (2005) 1059–1065, https://doi.org/10.1016/j.fuel.2005.01.016.
[31] S. Sriprathum, A. Maneedaeng, N. Klinkaew, E. Sukjit, Comprehensive analysis of properties of green diesel enhanced by fatty acid methyl esters, RSC Adv. 13 (2023) 31460–31469, https://doi.org/10.1039/D3RA06492A.
[32] G. Dhamodaran, R. Krishnan, Y.K. Pochareddy, H.M. Pyarelal, H. Sivasubramanian, A.K. Ganeshram, A comparative study of combustion, emission, and performance characteristics of rice-bran-, neem-, and cottonseed-oil biodiesels with varying degree of unsaturation, Fuel 187 (2017) 296–305, https://doi.org/10.1016/j.fuel.2016.09.062.
[33] A.A. Yusuf, F.L. Inambao, J.D. Ampah, The effect of biodiesel and CeO2 nanoparticle blends on CRDI diesel engine: a special focus on combustion, particle number, PM2.5 species, organic compound and gaseous emissions, J. King Saud Univ. - Eng. Sci. (2022), https://doi.org/10.1016/j.jksues.2021.12.003.
[34] R.K. Singh, S.K. Padhi, Characterization of jatropha oil for the preparation of biodiesel, Indian J. Nat. Prod. Resour. 8 (2006) 127–132.
[35] P. Goswami, T. Ohura, R. Suzuki, N. Koike, M. Watanabe, K.S. Guruge, Hazardous implications of halogenated polycyclic aromatic hydrocarbons in feedstuff: congener specificity and toxic levels in feed ingredients and feeds, Sci. Total Environ. 914 (2024) 169855, https://doi.org/10.1016/j.scitotenv.2023.169855.
[36] World Health Organization, Ambient (outdoor) air pollution, World Heal, Organ. Geneva (2021) 6–8. https://www.who.int/news-room/fact-sheets/detail/ambient-(outdoor)-air-quality-and-health (accessed March 16, 2024).
[37] HELCOM, Polyaromatic hydrocarbons (PAHs) and their metabolites, 1–17, www.helcom.fi, 2018.
[38] A. Pumpuang, N. Klinkaew, K. Wathakit, A. Sukhom, E. Sukjit, The influence of plastic pyrolysis oil on fuel lubricity and diesel engine performance, RSC Adv. 14 (2024) 10070–10087, https://doi.org/10.1039/D3RA08150H.
[39] Y.-C. Chien, Variations in amounts and potential sources of volatile organic chemicals in new cars, Sci. Total Environ. 382 (2007) 228–239, https://doi.org/10.1016/j.scitotenv.2007.04.022.
[40] W. Huang, M. Lv, X. Yang, Long-term volatile organic compound emission rates in a new electric vehicle: influence of temperature and vehicle age, Build. Environ. 168 (2020) 106465, https://doi.org/10.1016/j.buildenv.2019.106465.
[41] A.A. Yusuf, H. Dandakouta, I. Yahuza, D.A. Yusuf, M.A. Mujtaba, A.S. El-Shafay, M. E.M. Soudagar, Effect of low CeO2 nanoparticles dosage in biodiesel-blends on combustion parameters and toxic pollutants from common-rail diesel engine, Atmos. Pollut. Res. 13 (2022) 101305, https://doi.org/10.1016/j.apr.2021.101305.
[42] L. Zhu, W. Zhang, W. Liu, Z. Huang, Experimental study on particulate and NOx emissions of a diesel engine fueled with ultra low sulfur diesel, RME-diesel blends and PME-diesel blends, Sci. Total Environ. 408 (2010) 1050–1058, https://doi.org/10.1016/j.scitotenv.2009.10.056.
[43] G. Pehnec, I. Jakovljević, Carcinogenic potency of airborne polycyclic aromatic hydrocarbons in relation to the particle fraction size, Int. J. Environ. Res. Public Health. 15 (2018) 2485, https://doi.org/10.3390/ijerph15112485.
[44] B. Bukowska, K. Mokra, J. Michałowicz, Benzo[a]pyrene—environmental occurrence, human exposure, and mechanisms of toxicity, Int. J. Mol. Sci. 23 (2022) 6348, https://doi.org/10.3390/ijms23116348.
[45] A.A. Yusuf, F.L. Inambao, Effect of low bioethanol fraction on emissions, performance, and combustion behavior in a modernized electronic fuel injection engine, Biomass Convers. Biorefinery 11 (2021) 885–893, https://doi.org/10.1007/s13399-019-00519-w.
[46] E. David, V.-C. Niculescu, Volatile organic compounds (VOCs) as environmental pollutants: occurrence and mitigation using nanomaterials, Int. J. Environ. Res. Public Health. 18 (2021) 13147, https://doi.org/10.3390/ijerph182413147.
[47] J. Shuai, S. Kim, H. Ryu, J. Park, C.K. Lee, G.-B. Kim, V.U. Ultra, W. Yang, Health risk assessment of volatile organic compounds exposure near Daegu dyeing industrial complex in South Korea, BMC Publ. Health 18 (2018) 528, https://doi.org/10.1186/s12889-018-5454-1.
[48] J. Xue, T.E. Grift, A.C. Hansen, Effect of biodiesel on engine performances and emissions, Renew. Sustain. Energy Rev. 15 (2011) 1098–1116, https://doi.org/10.1016/j.rser.2010.11.016.
[49] M. Alam, J. Song, R. Acharya, A. Boehman, K. Miller, Combustion and Emissions Performance of Low Sulfur, Ultra Low Sulfur and Biodiesel Blends in a DI Diesel Engine, 2004, https://doi.org/10.4271/2004-01-3024.
[50] A. Sethin, Y.M. Oo, J. Thawornprasert, K. Somnuk, Effects of blended diesel–biodiesel fuel on emissions of a common rail direct injection diesel engine with different exhaust gas recirculation rates, ACS Omega 9 (2024) 20906–20918, https://doi.org/10.1021/acsomega.3c10125.
[51] B. Wang, W.H. Or, S.C. Lee, Y.C. Leung, B. Organ, K.F. Ho, Characteristics of particle emissions from light duty diesel vehicle fueled with ultralow sulphur diesel and biodiesel blend, Atmos. Pollut. Res. 12 (2021) 101169, https://doi.org/10.1016/j.apr.2021.101169.
[52] S. Feng, D. Gao, F. Liao, F. Zhou, X. Wang, The health effects of ambient PM2.5 and potential mechanisms, Ecotoxicol. Environ. Saf. 128 (2016) 67–74, https://doi.org/10.1016/j.ecoenv.2016.01.030.
[53] D.T. Silverman, C.M. Samanic, J.H. Lubin, A.E. Blair, P.A. Stewart, R. Vermeulen, J.B. Coble, N. Rothman, P.L. Schleiff, W.D. Travis, R.G. Ziegler, S. Wacholder, M. D. Attfield, The diesel exhaust in miners study: a nested case-control study of lung cancer and diesel exhaust, J. Natl. Cancer Inst. 104 (2012) 855–868, https://doi.org/10.1093/jnci/djs034.
[54] M. Shen, Particulate matter emissions from partially premixed combustion with diesel, Gasoline and Ethanol. Ph.D dissertation, Faculty of Eng., Lund Univ, 2016, pp. 1–93.